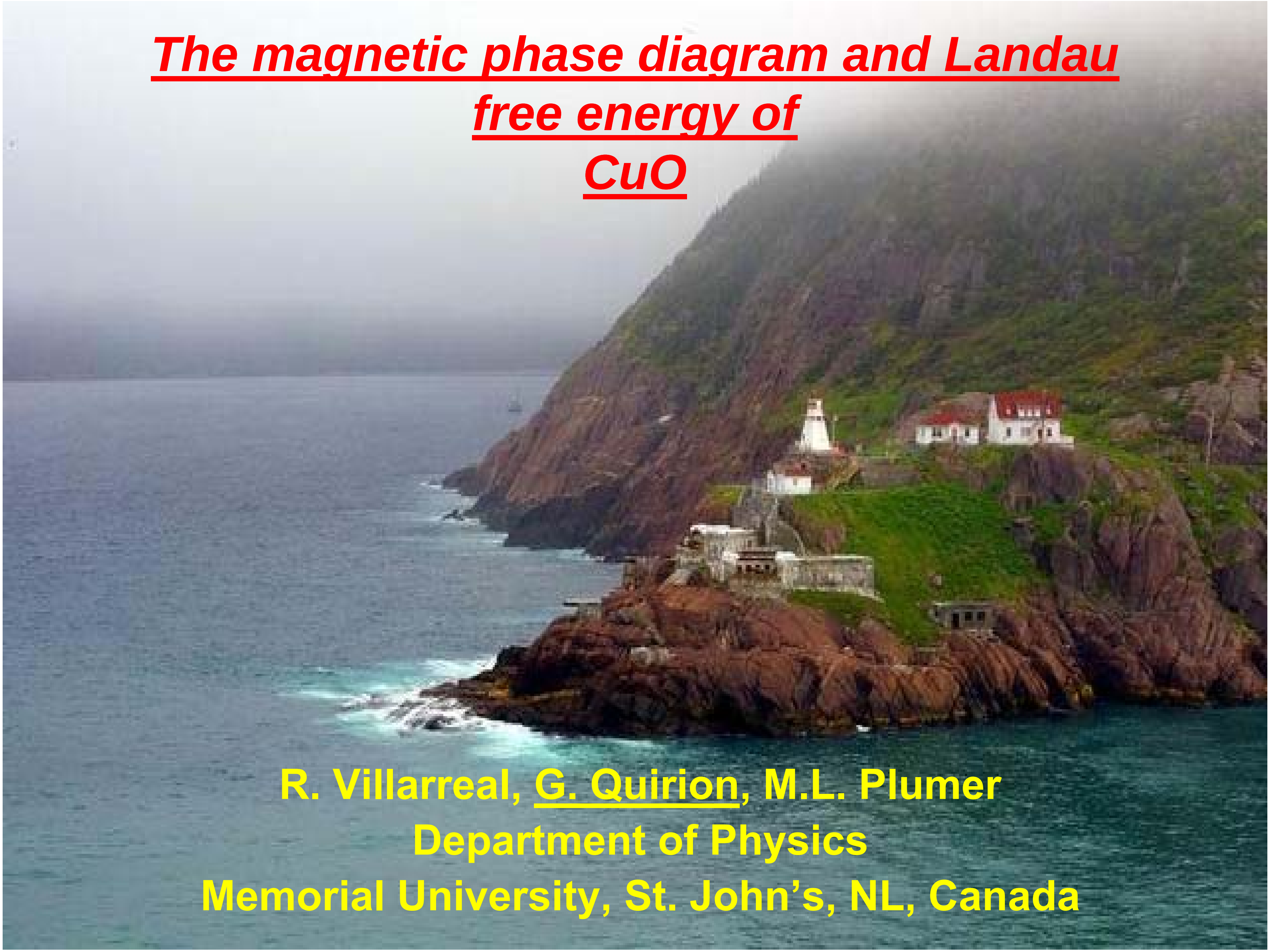

# ***The magnetic phase diagram and Landau free energy of CuO***

**R. Villarreal, G. Quirion, M.L. Plumer**
**Department of Physics**
**Memorial University, St. John’s, NL, Canada**

## ***Collaborators***


**M. Poirier**
**Département de Physique**
**Université de Sherbrooke, Sherbrooke, QC, Canada**



T. Usui, T. Kimura
Division of Materials Physics, Osaka University,
Osaka, Japan

# Spin-Driven Multiferroics

- •Ferroelectric
  - -> transition metal ions with empty d shell
- •Magnetism
  - -> requires partially filled  shell

} ferroelectricity and magnetism exclude each other

10 years ago

$TbMnO_3$ and $DyMnO_3$ -> ferroelectric order driven by spiral magnetic order

renews the interest for the search of magnetoelectric materials

**DM interaction**

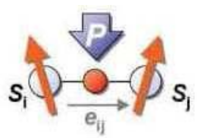


$$\mathbf{P}_{ij} = A_0 \cdot \mathbf{e}_{ij} \times (\mathbf{S}_i \times \mathbf{S}_j)$$

Wave vector Q

Cycloidal

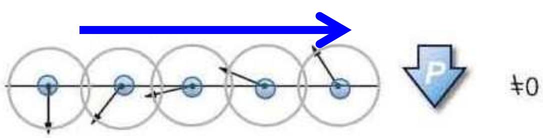


**P ⊥ Q**

**Other mechanism**

Proper Screw

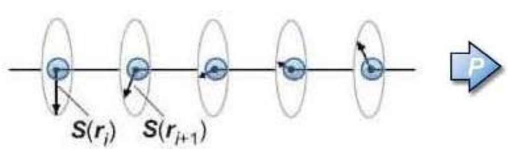


**P // Q**

$CuFeO_2$, $CuCrO_2$

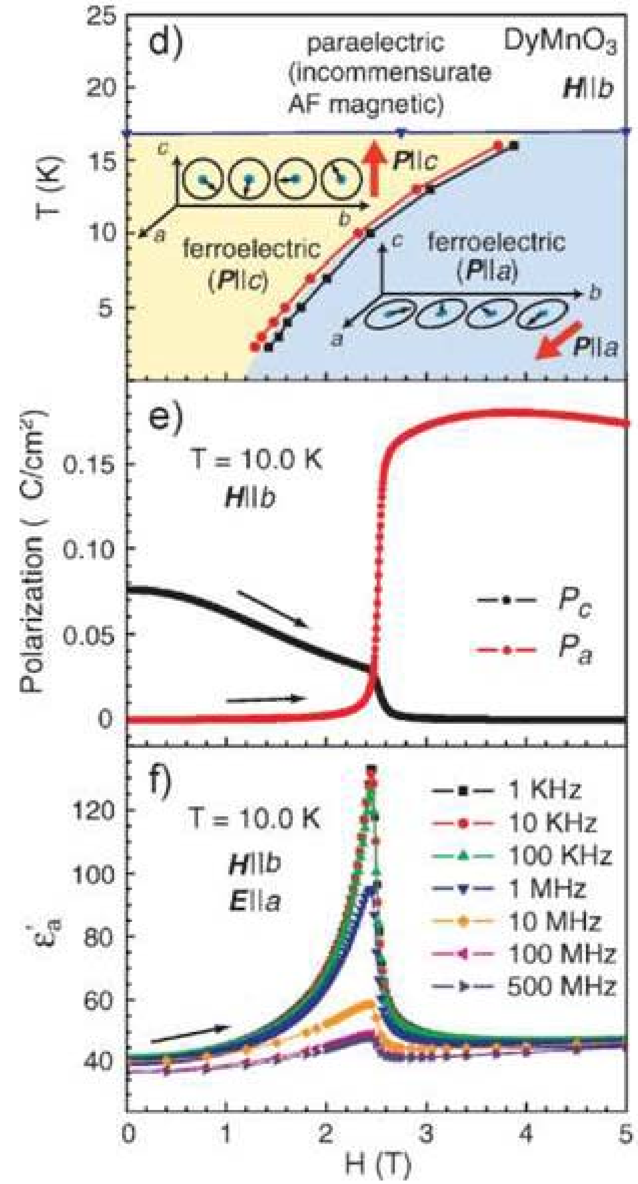


F. Kagawa, PRL, 102, 057604, 2009.

# Spin-Driven Multiferroics

As spiral magnetic orders } arise from spin frustration

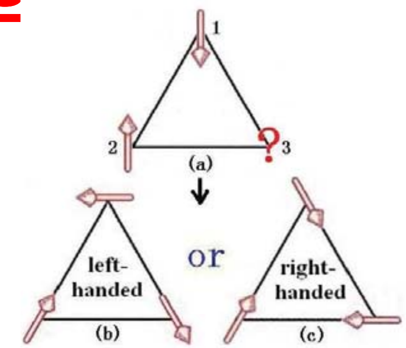


Table 2. A list of multiferroics with spiral spin-order-induced ferroelectricity.

| Compound | Crystal structure | Magnetic ions | Spiral spin wave vector $q$ | Ferroelectric temperature (K) | Spontaneous polarization ($\mu$C m$^{-2}$) |
|---|---|---|---|---|---|
| $LiCu_2O_2$ | Orthorhombic (*Pnma*) | $Cu^{2+}$ | (0.5, 0.174, 0) | $<23$ | $P_c = 4$ |
| $LiCuVO_4$ | Orthorhombic (*Pnma*) | $Cu^{2+}$ | (0, 0.53, 0) | $<3$ | $P_a = 20$ |
| $Ni_3V_2O_8$ | Orthorhombic (*mmm*) | $Ni^{2+}$ | (0.28, 0, 0) | 3.9–6.3 | $P_b = 100$ |
| $RbFe(MoO_4)_2$ | Triangular ($P\bar{3}m1$) | $Fe^{3+}$ | (1/3, 1/3, 0.458) | $<3.8$ | $P_c = 5.5$ |
| $CuCrO_2$, $AgCrO_2$ | Delafossite ($R\bar{3}m$) | $Cr^{3+}$ | (1/3, 1/3, 0) | $<24$ | 30[b] |
| $NaCrO_2$, $LiCrO_2$ | Ordered sock salt ($R\bar{3}m$) | $Cr^{3+}$ | (1/3, 1/3, 0) and (−2/3, 1/3, 1/2) | $<60$ | Antiferroelectricity |
| $CuFeO_2$ | Delafossite ($R\bar{3}m$) | $Fe^{3+}$ | ($b$, $b$, 0) $b = 0.2$–0.25 | $<11$ | $P = 300$ ($\perp$c) (H=6-13T)[a] |
| $Cu(Fe,Al/Ga)O_2$ Al/Ga = 0.02 | Delafossite ($R\bar{3}m$) | $Fe^{3+}$ | ? | $<7$ | $P_{[110]} = 50$ |
| $RMnO_3$ (R = Tb,Dy) | Orthorhombic (*Pbnm*) | $Mn^{3+}$ | (0, $k$, 1) $k = 0.2$–0.39 | $<28$ | $P_c = 500$ |
| $CoCr_2O_4$ | Cubic spinel ($m3m$) | $Cr^{3+}$ | ($b$, $b$, 0) $B = 0.63$ | $<26$ | $P_c = 2$ |
| $AMSi_2O_6$ ($A$=Na,Li; $M$ = Fe,Cr) | Monoclinic ($C2/c$) | $Fe^{3+}$ $Cr^{3+}$ | ? | $<6$ | $P_b = 14$ |
| $MnWO_4$ | Monoclinic ($Pc/2$) | $Mn^{2+}$ | (−0.21, 0.5, 0.46) | 7–12.5 | $P_b = 55$ |
| CuO | Monoclinic ($C2/c$) | $Cu^{2+}$ | (0.506, 0, −0.843) | 213–230 | $P_b = 150$ |
| $(Ba,Sr)_2Zn_2Fe_{12}O_{22}$ | Rhomboheral Y-type hexaferrite | $Fe^{3+}$ | (0, 0, 3$d$) $0 < d < 1/2$ | $<325$ | 150 ($H = 1$ T)[a] |
| $Ba_2Mg_2Fe_{12}O_{22}$ | Rhomboheral Y-type hexaferrite | $Fe^{3+}$ | //[001] | $<195$ | $P_{[120]}$=80 ($H = 0.06$–4 T)[a] |
| $ZnCr_2Se_4$ | Cubic spinel | $Cr^{3+}$ | ($b$, 0, 0) | $<20$ | –[a] |
| $Cr_2BeO_4$ | Orthorhombic | $Cr^{3+}$ | (0, 0, $b$) | $<28$ | 3[b] |

[a]An external magnetic field is needed to induce the spiral spin order and then the ferroelectricity.
[b]Polycrystalline samples.

# CuO

**monoclinic *C2/c* (2/*m*)**

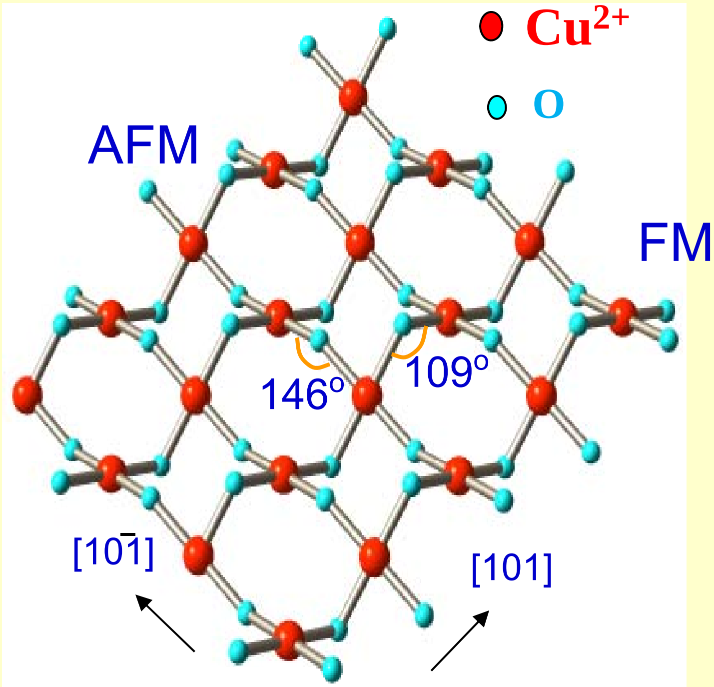


The structure can be considered as being composed of Cu-O chains running along [101] and [10-1] directions.

Mizuno, Tohyama, Maekawa et al. PRB 57, 5326 (1998);
Shimizu et al. JPSJ 72, 2165 (2003),

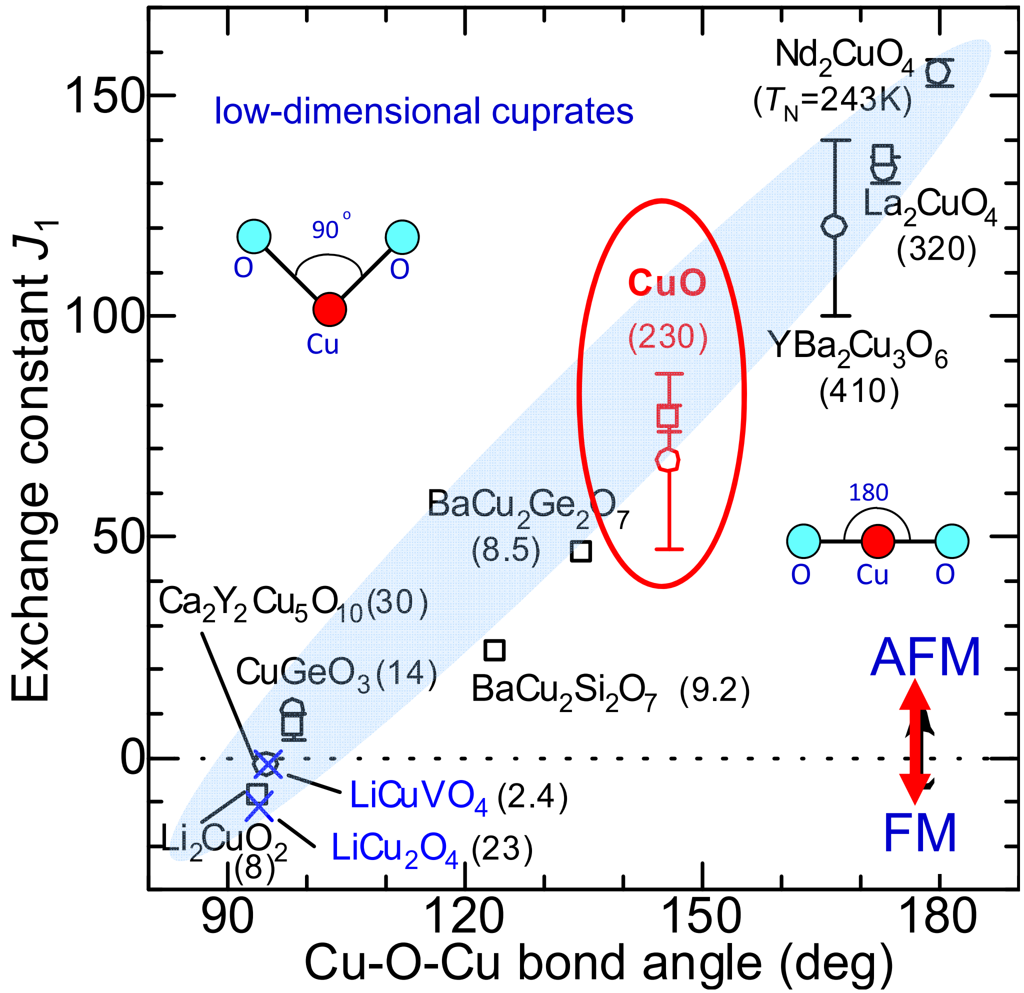

# Magnetic and Electric Properties

## Cu0

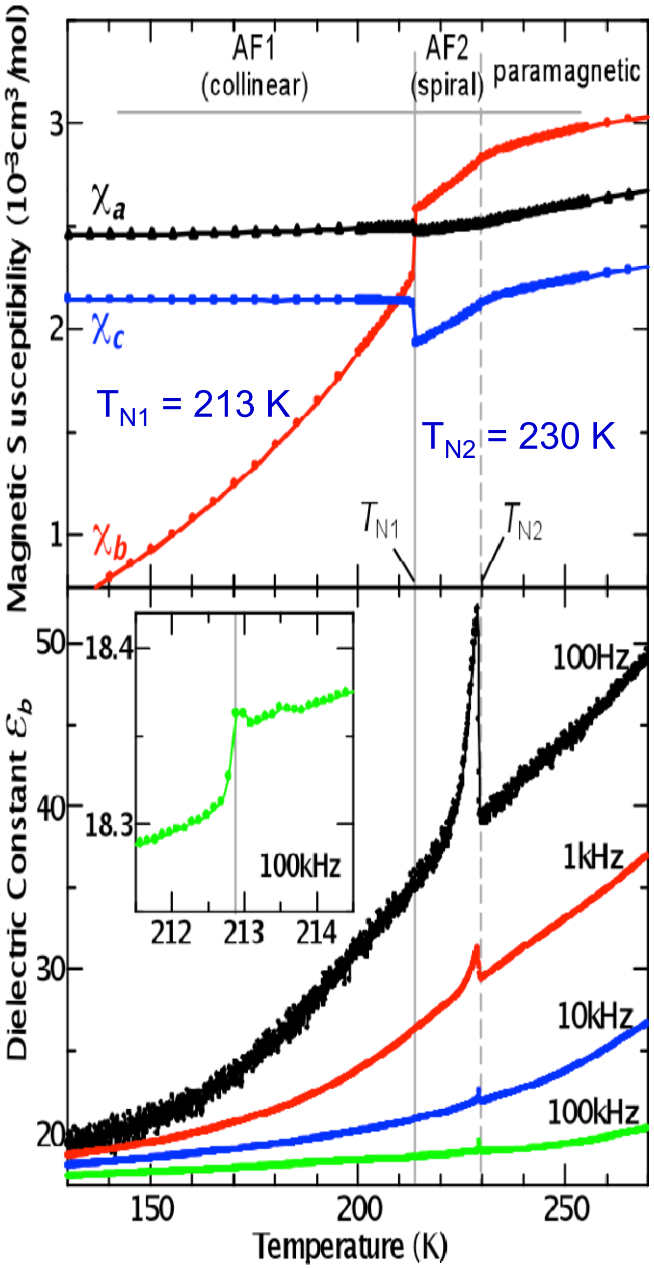


Spontaneous Polarization along b-axis

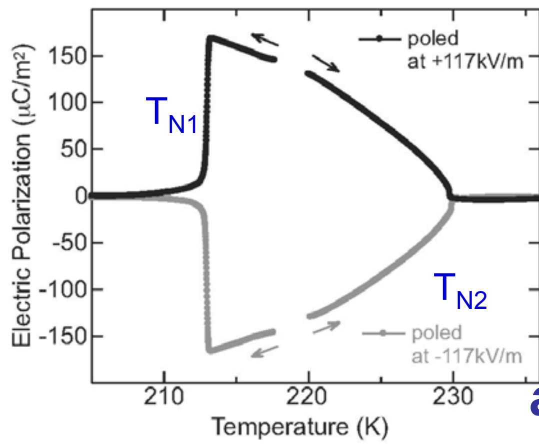


**T. Kimura et al., Nature Materials, 7, 291 (2008)**

## Spin Configuration

**AF2 (spiral)**

$T_{N2}$ = 230 K

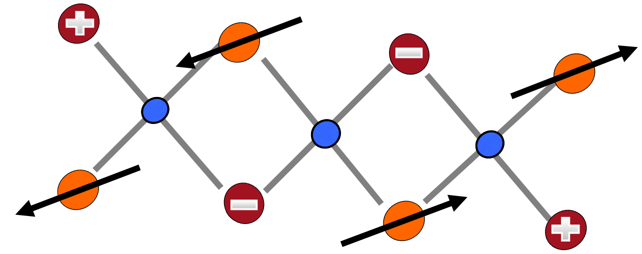

**$Q_{ICM}$ = [0.506 0 -0.483]**

**AF1 (collinear)**

$T_{N1}$ = 213 K

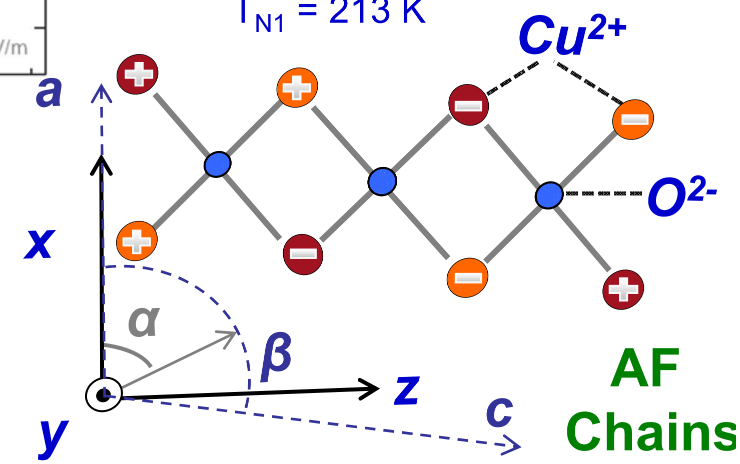


**$Q_{CM}$ = [0.5 0 -0.5]**

# Sound Velocity Measurements

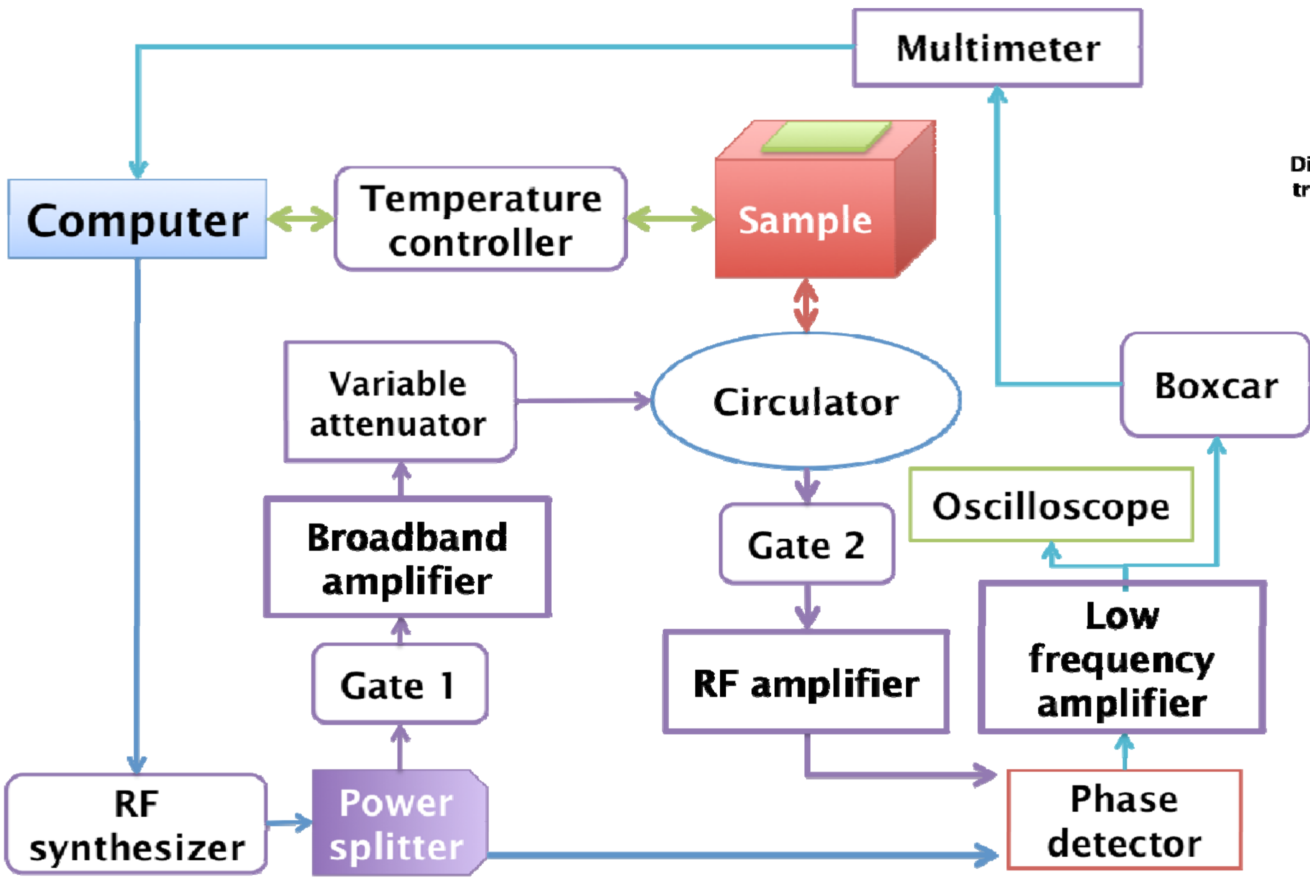


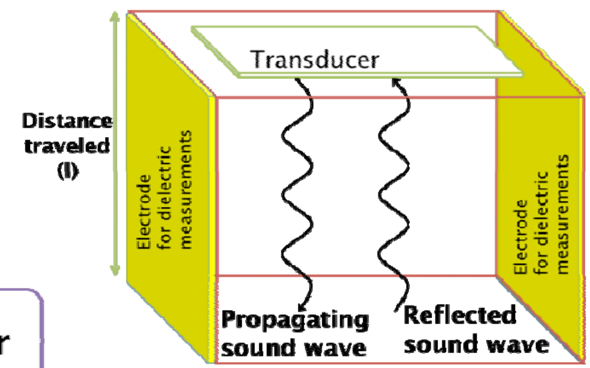


$$V = \sqrt{\frac{C_{eff}}{\rho}} = \frac{2L}{\Delta t}$$

$$\frac{dV}{V} \cong \frac{df}{f}$$

Ultrasonic interferometer
higher resolution

$\Delta V/V \sim 10^{-6}$

# Sound Velocity Measurements

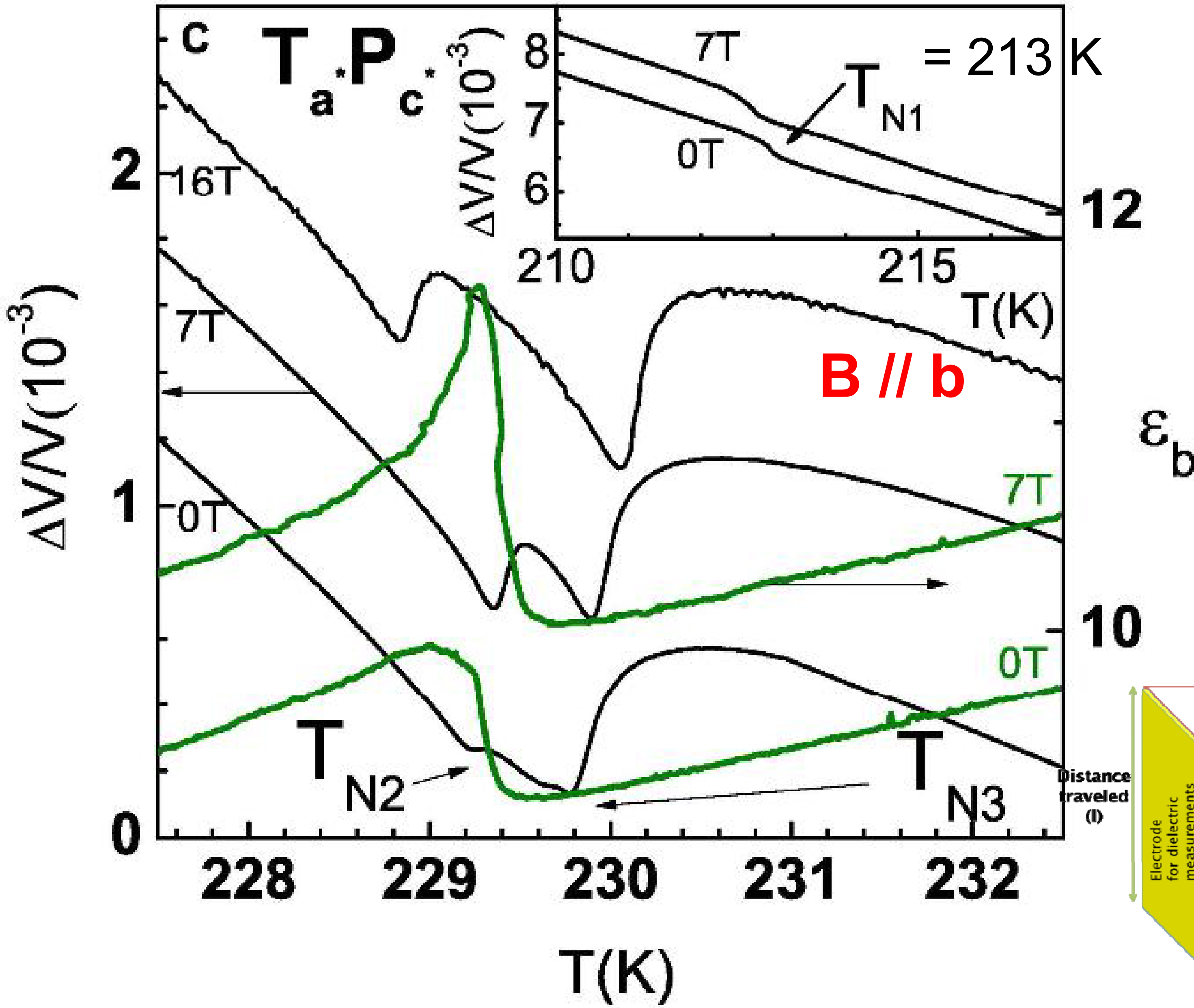


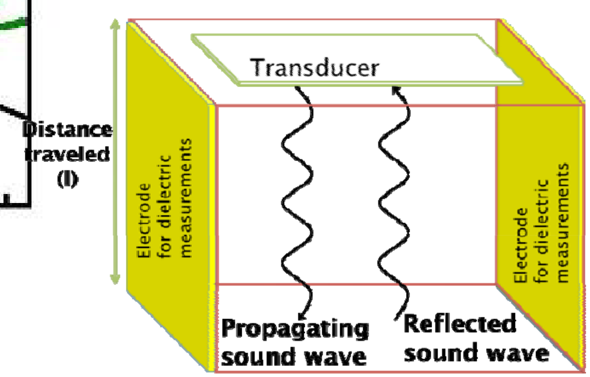

# Magnetic Phase Diagram of CuO

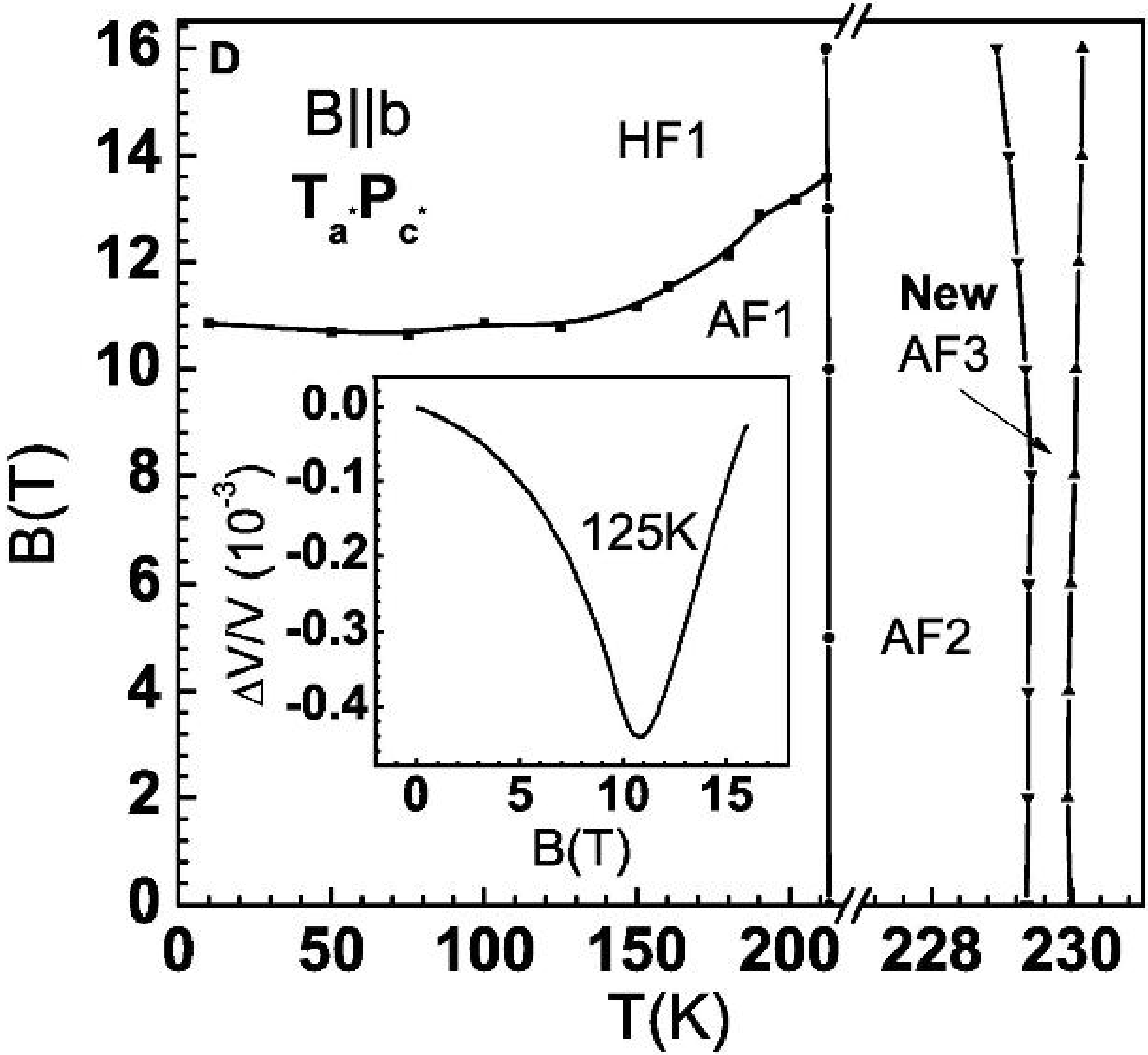

# Landau Model CuO

Landau Free Energy: $F_L = F_{2I} + F_{2A} + F_4 + F_Z$

Second Order Isotropic Contribution:

$$F_{2I} = \frac{1}{2V^2}\int d\vec{r}_1 d\vec{r}_2 A(\vec{r}_1, \vec{r}_2) s(\vec{r}_1)\cdot s(\vec{r}_2)$$

Second Order Single-ion Anisotropic Contribution:

$$F_{2A} = \frac{1}{2V}\int d\vec{r}\left\{D_y(\vec{r})s_y(\vec{r})s_y(\vec{r}) + D_z(\vec{r})s_z(\vec{r})s_z(\vec{r}) + D_{xz}(\vec{r})s_x(\vec{r})s_z(\vec{r})\right\}$$

Fourth Order Isotropic Contribution:

$$F_4 = \frac{1}{4V^4}\int d\vec{r}_1 d\vec{r}_2 d\vec{r}_3 d\vec{r}_4 \left\{B(\vec{r}_1, \vec{r}_2, \vec{r}_3, \vec{r}_4)\ s(\vec{r}_1)\cdot s(\vec{r}_2)\ s(\vec{r}_3)\cdot s(\vec{r}_4)\right.$$

# Spin Density

Local Spin Density: $$\vec{s}(\vec{r}) = \frac{V}{N}\sum_R \vec{\rho}(\vec{r})\ \delta(\vec{r}-\vec{R})$$

Non-local Spin Density $$\vec{\rho}(r) = \vec{m} + \vec{S}e^{i\vec{Q}\cdot\vec{r}} + \vec{S}^* e^{-i\vec{Q}\cdot\vec{r}}$$

**Q wave vector associated with the spin configuration**

where $$\vec{S} = \vec{S}_1 + i\,\vec{S}_2$$

**Describes non-collinear spin configuration**

$$\vec{S}_1 = S\cos\beta\left[\cos\gamma\ \hat{y} + \sin\gamma\ \hat{\rho}_2\right]$$

$$\vec{S}_2 = S\sin\beta\left[\cos\theta\ \hat{\rho}_1 + \sin\theta\ (\cos\gamma\ \hat{y} + \sin\gamma\ \hat{\rho}_2)\right]$$

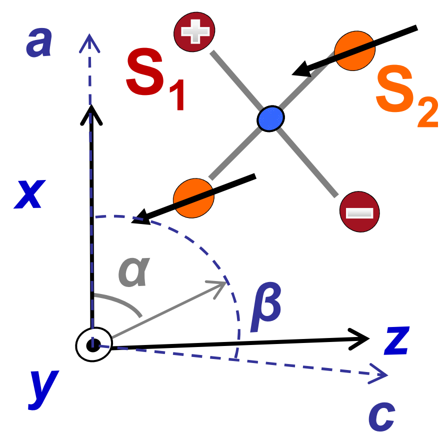


$$\hat{\rho}_1 = \cos\alpha\ \hat{x} + \sin\alpha\ \hat{z}$$

$$\hat{\rho}_2 = -\sin\alpha\ \hat{x} + \cos\alpha\ \hat{z}$$

two orthogonal unit vectors in the ac-plane

# Wave Vector Q

Second Order Isotropic Contribution:

$$F_{2I} = \frac{1}{2V^2}\int d\vec{r}_1 d\vec{r}_2 A(\vec{r}_1,\vec{r}_2)s(\vec{r}_1)\cdot s(\vec{r}_2)$$

$$F_{2I} = \frac{1}{2}\tilde{A}m^2 + A_Q S^2$$

where

$A_Q = a\,T + J(Q)$

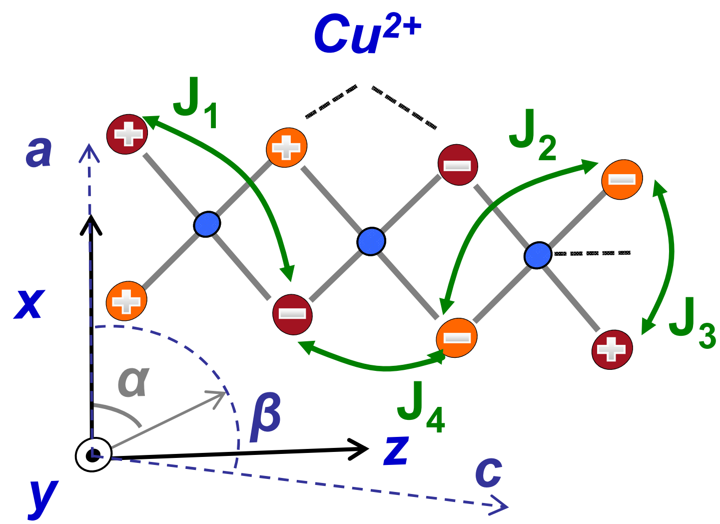


$J(Q) = 2\,[J_1f_1(Q) + J_2f_2(Q) + J_3f_3(Q) + J_4f_4(Q)]$

$f_1(Q) = \cos(\pi\, q_a - \pi\, q_c)$

$f_2(Q) = \cos(\pi\, q_a + \pi\, q_c)$

$f_3(Q) = \cos(\pi\, q_a - \pi\, q_b) + \cos(\pi\, q_a + \pi\, q_b)$

$f_4(Q) = \cos(\pi\, q_b - \pi\, q_c) + \cos(\pi\, q_b + \pi\, q_c)$

# *Wave Vector Q*

## Antiferromagnetic States
## ($J_1$ = 1)

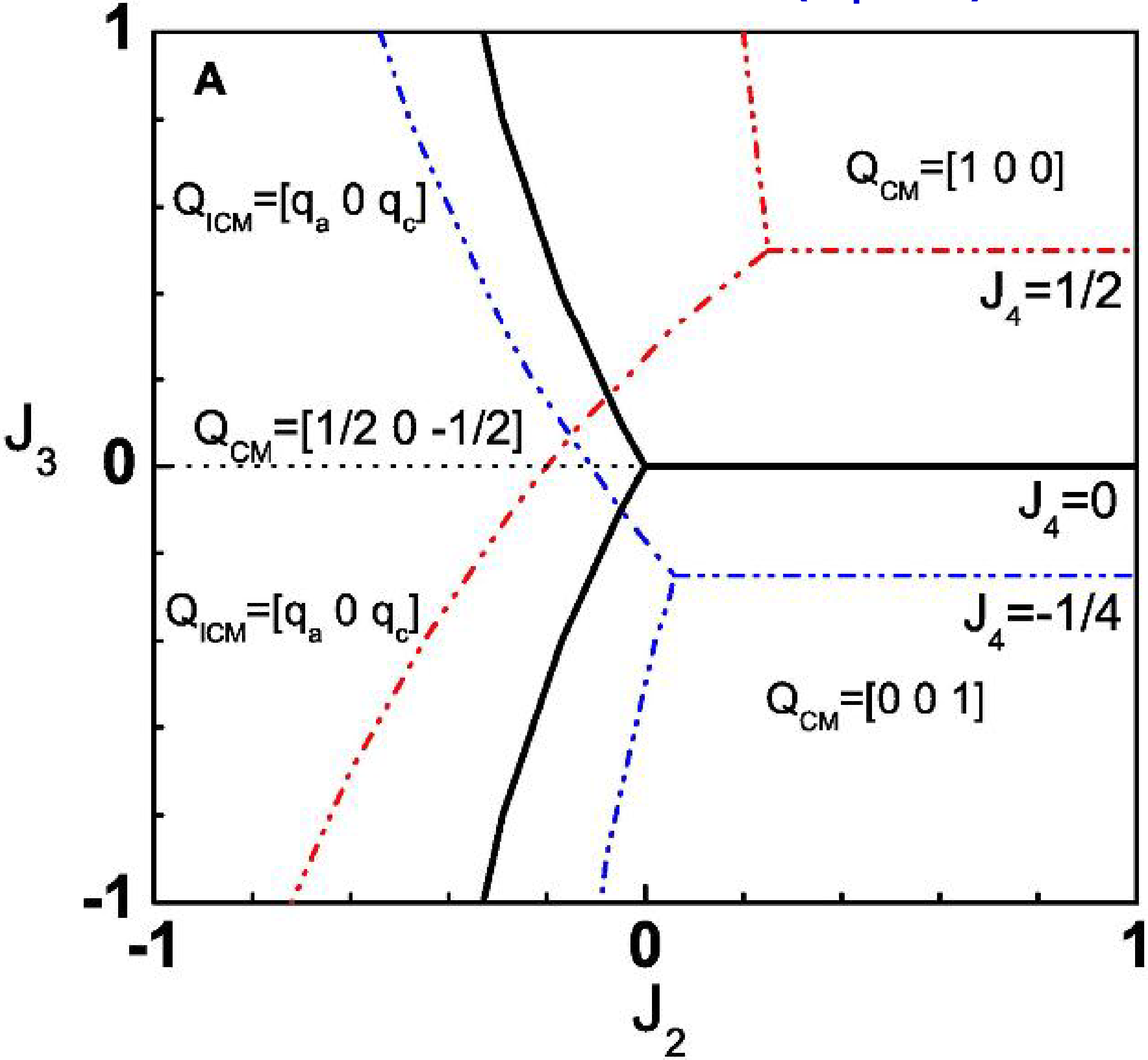


$Q_{ICM}$ = [0.506 0 − 0.483]

**$J_2/J_1 = -0.3$,**
**$J_3/J_1 = 0.017$,**
**$J_4/J_1 = 0$**

**leading to**
**$J_Q/J_1 = -2.6$**

# Magnetic Phase Diagram of CuO

$$F_L = A_Q S^2 - D_{yQ}\left|S_y\right|^2 - D_{zQ}\left|S_z\right|^2 + D_{xzQ} S_x S_z + B_1 S^4 + \frac{1}{2} B_2 \left|\vec{S}\cdot\vec{S}\right|^2 + \frac{1}{4} B_U \left[\left(\vec{S}\cdot\vec{S}\right)^2 + c.c\right] \Delta_{4Q,G}$$

$$+\frac{1}{2} A_o m^2 + \frac{1}{4} B_3 m^4 + 2B_4 \left|\vec{m}\cdot\vec{S}\right|^2 + B_5 m^2 S^2 - H\cdot m$$

$A_Q = a\,(T - T_Q)$

## Numerical Predictions

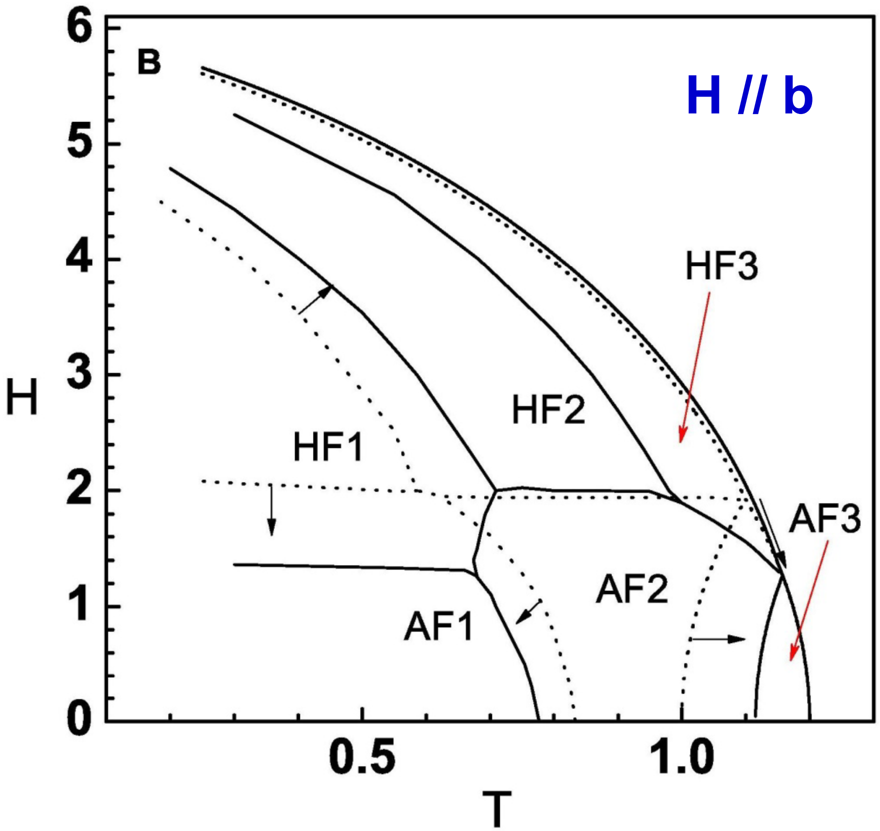


## Experimental Results

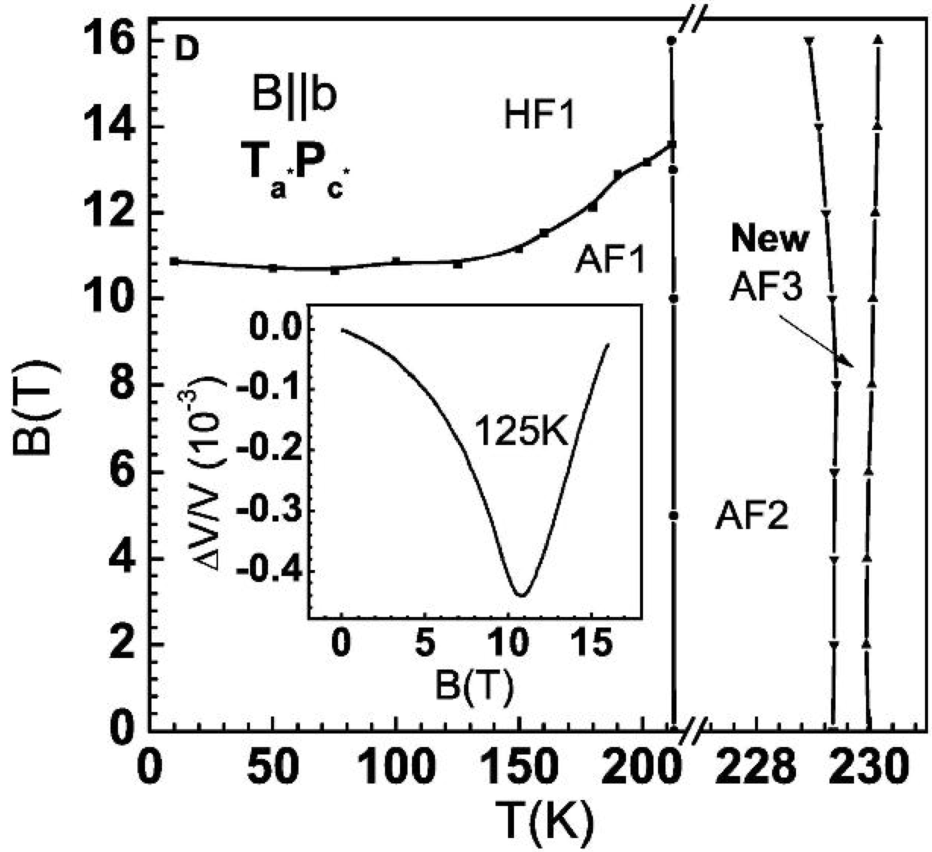

# Spin Configurations

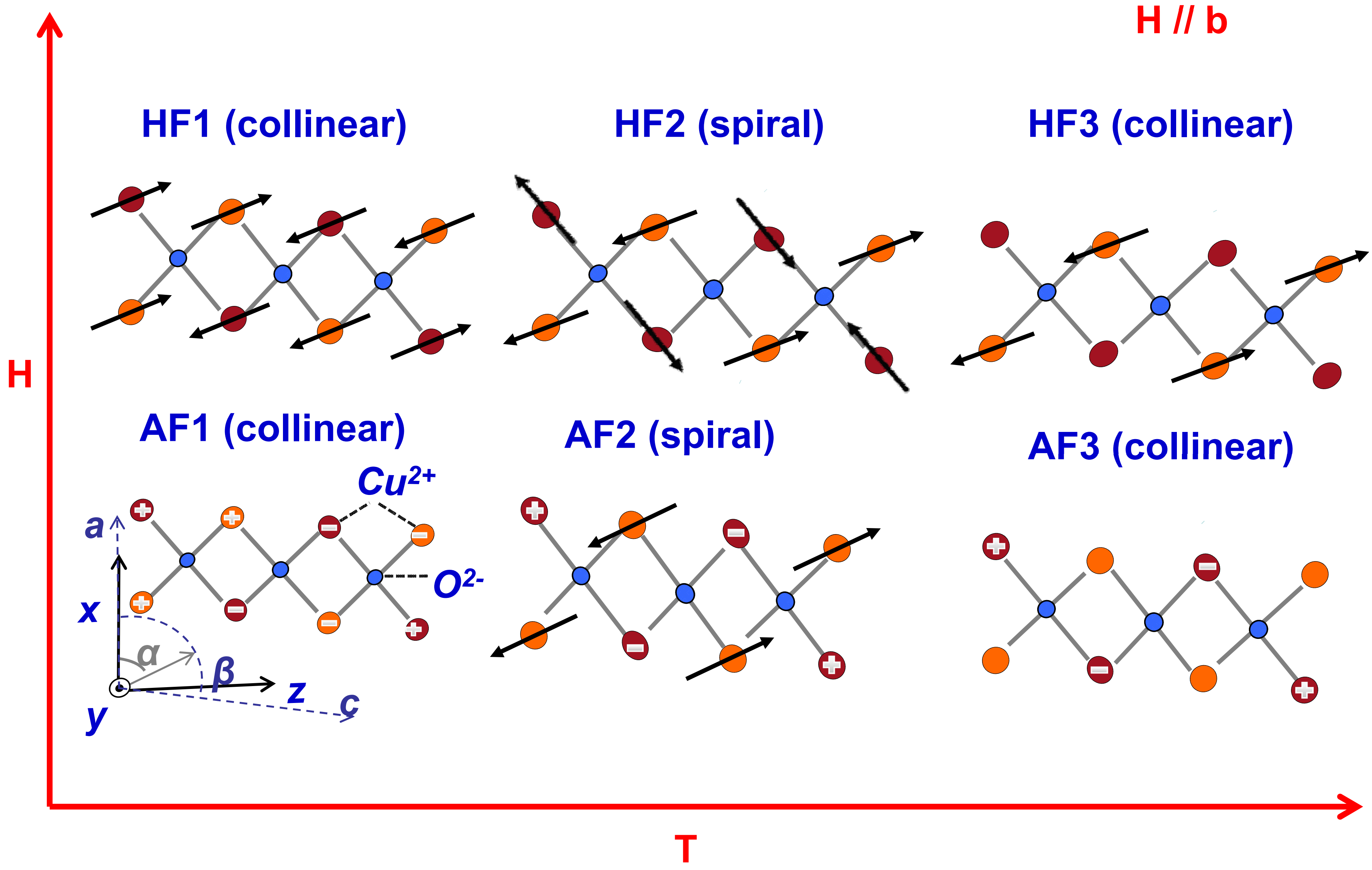

# Conclusions

*•new collinear phase (AF3) detected between the PM and the spiral phase (AF2).*

*• for B // b, we also observe a spin-flop phase (HF1) at low temperatures.*

*• Complementary dielectric measurements confirm that magnetoelectric effects exist only in the spiral phase (AF2).*

*▪ the existence of the intermediate phase AF3 is supported by our Landau model .*

*▪The model predicts additional phase transitions possibly at higher fields.*

*•Finally, the proposed model is potentially useful for the description of other monoclinic multiferroic systems, such as $MnWO_4$ and $AMSi_2O_6$.*

## References


- **R. Villarreal et al., cond-mat : arXiv:1205.5229v1 (2012)**
- **T. Kimura et al., Nature Materials, 7, 291, (2008)**

# $MnWO_4$

**V. Felea et al., J. Phys.: Cond. Matter 23, 216001 (2011).**